No.342 (#19 – 23)

19. A multi-line study of the filamentary infrared dark cloud G351.78-0.54

20. Evolution of the atomic component in protostellar outflows

21. A study of the photometric and spectroscopic variations of the prototypical FU Orionis-type star V1057 Cyg

22. The *Gaia* view of the Cepheus flare

23. Molecular Cloud Cores with High Deuterium Fractions: Nobeyama Mapping Survey

A multi-line study of the filamentary infrared dark cloud G351.78-0.54

Show affiliations

Ryabukhina, O. L. ; Zinchenko, I. I.

We present results of a multi-line study of the filamentary infrared dark cloud G351.78-0.54 in the 1.3 and 0.8 mm wavelength bands. The lines of the three isotopologues of carbon monoxide CO, N_2H^+, CH_3CCH and HNCO were observed. The aim was to study the general structure of the filamentary cloud, its fragmentation and physical parameters with the emphasis on properties of dense clumps in this cloud. Several dense clumps are identified from the N_2H^+ (3-2) data, their masses and virial parameters are determined using the $C^{18}O$ (2-1) line. Temperatures of some clumps are estimated from the CH_3CCH and HNCO data. Almost all clumps appear to be gravitationally unstable. The density estimates obtained from the $C^{18}O$ (3-2)/(2-1) and N_2H^+ (3-2)/(1-0) intensity ratios are in the range $n \sim (0.3 - 3) \times 10^5$ cm^{-3}. The HNCO emission is detected exclusively toward the first clump which contains the luminous IR source IRAS 17233-3606, and indicates an even higher density. It is observed in the outflow, too. The velocity shift of the higher excitation HNCO lines may indicate a movement of the hot core relative the surrounding medium. In some clumps there is a velocity shift ~1 km s^{-1} between N_2H^+ (3-2) and CO isotopologues. The large widths of the N_2H^+ (3-2) line in the clumps indicate an increase of the velocity dispersion in their dense interiors, which may be related to the star formation process. The N_2H^+ abundance drops toward the luminous IR source.

ターゲット：G351.78–0.54

- フィラメント状の赤外線暗黒星雲

観測：

- APEX電波望遠鏡 (2010 – 2017)
- CO, N_2H, CH_3CCH, HNCO輝線

フィラメント

- M_{tot} ~ 1800 [$M_\odot$]
- M_{line} = 529 [$M_\odot$/pc] ~ $M_{line,virial}$ → 分裂

6つの高密度クランプ

- 5/6が重力不安定
- 高密度領域の高い速度分散を確認
  → ケプラー回転 or 中心落下運動

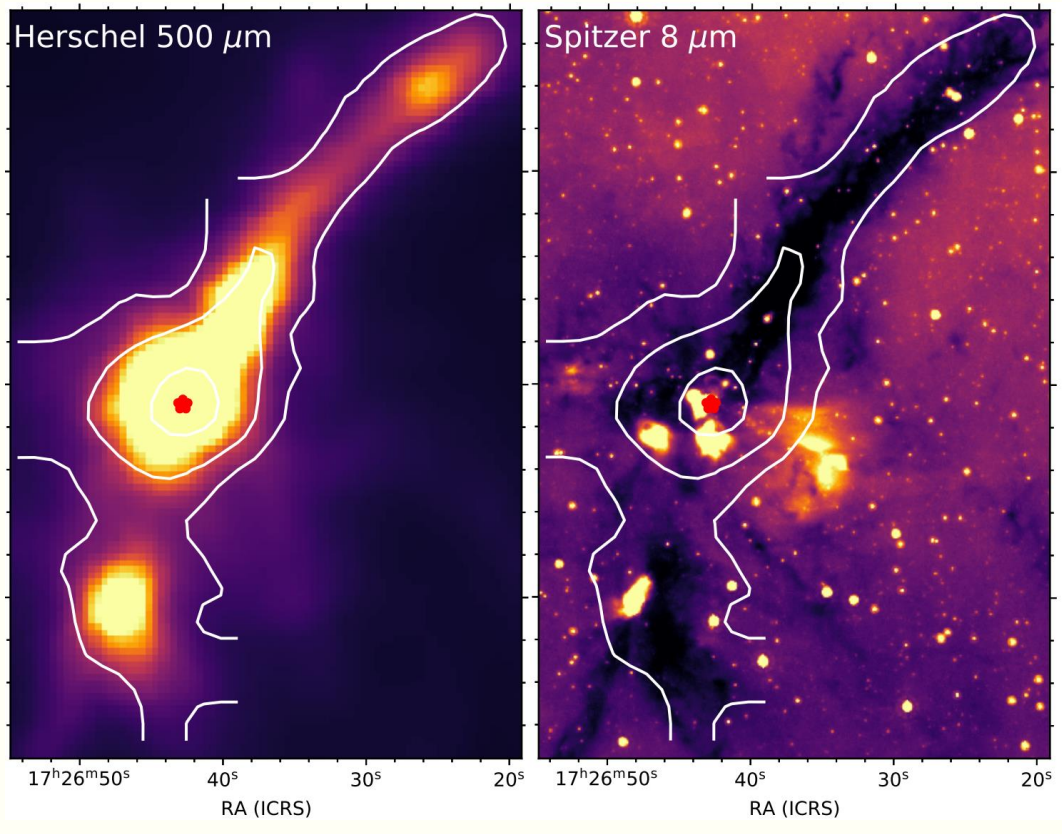

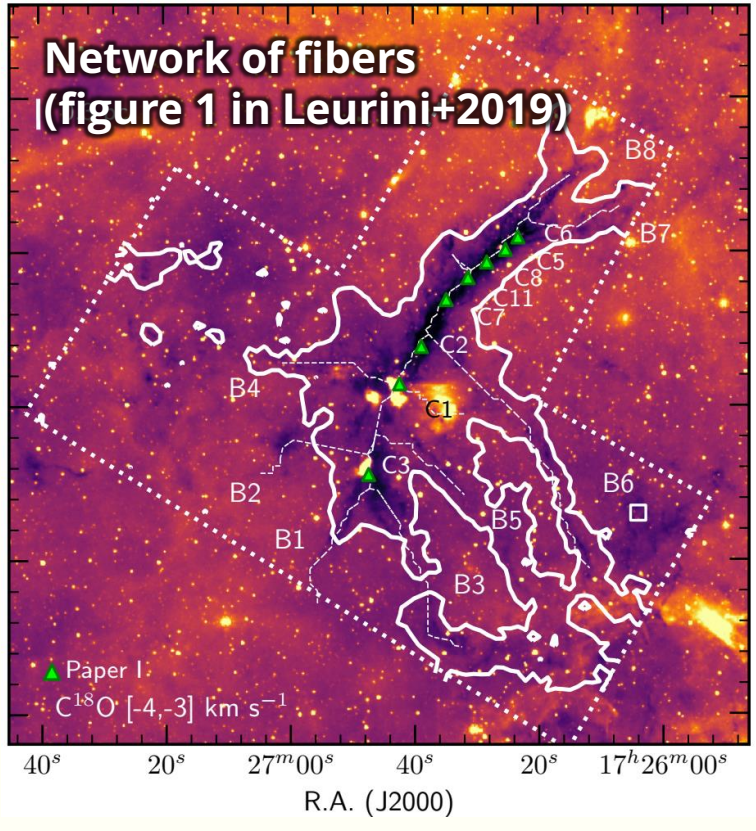

- フィラメントの {距離, 長さ, 幅, 質量} = {0.7–1 [kpc], 4.6 [pc], 0.2 [pc], >1300 [$M_\odot$]}
- 星雲の中央に、明るい赤外線天体であるIRAS17233-3606が存在する (左図の赤点)。
- 12個のクランプが同定 (Leurini+2011)。星形成段階がそれぞれ異なる。
- 分子輝線の広がったプロファイルは、膨張HII領域による衝撃波圧縮によるものと考えられているが、衝撃波の駆動要因は特定できていない。

装置：APEX (Atacama Pathfinder Experiment) 電波望遠鏡
期間：2010-2017
観測輝線： CO, N_2H, CH_3CCH, HNCO (右表)

利用したパッケージ一覧
輝線のパラメータ：Cologne Database for Molecular Spectroscopy (CDMS), Jet Propulsion Laboratory (JPL) catalog
輝線データ解析　：CLASS program from the GILDAS
イメージ解析　　：MIRIAD, Astropy
分子クランプ同定　　：Starlink
CH3CCH遷移の回転温度推定　　：CASSIS
N2H+(3-2)輝線の超微細構造計算：PySpecKit
13CO, C18O, N2H+の励起解析　：Radex

Molecule	Transition	Frequency (GHz)	E_l (K)
CO	2–1	230.538	5.53
^{13}CO	2–1	220.399	5.29
	3–2	330.588	15.87
$C^{18}O$	2–1	219.560	5.27
	3–2	329.331	15.80
N_2H^+	3–2	279.512	13.41
CH_3CCH	13_0–12_0	222.166	63.98
	13_1–12_1	222.163	71.18
	13_2–12_2	222.150	92.78
	13_3–12_3	222.129	128.77
	13_4–12_4	222.099	179.17
	13_5–12_5	222.061	243.97
	13_6–12_6	222.014	323.17
HNCO	$10_{0,10}$–$9_{0,9}$	219.798	47.47
	$10_{1,10}$–$9_{1,9}$	218.981	90.57
	$10_{1,9}$–$9_{1,8}$	220.585	90.92
	$10_{2,9}$–$9_{2,8}$	219.734	217.74
	$10_{2,8}$–$9_{2,7}$	219.737	217.74
	$10_{3,8}$–$9_{3,7}$	219.657	422.42
	$10_{3,7}$–$9_{3,6}$	219.657	422.42
	$15_{0,15}$–$14_{0,14}$	329.664	110.76
	$15_{2,14}$–$14_{2,13}$	329.573	281.01
	$15_{2,13}$–$14_{2,12}$	329.585	281.01
	$15_{3,13}$–$14_{3,12}$	329.460	485.67
	$15_{3,12}$–$14_{3,11}$	329.460	485.67
	$15_{4,12}$–$14_{4,11}$	329.295	761.39
	$15_{4,11}$–$14_{4,10}$	329.295	761.39

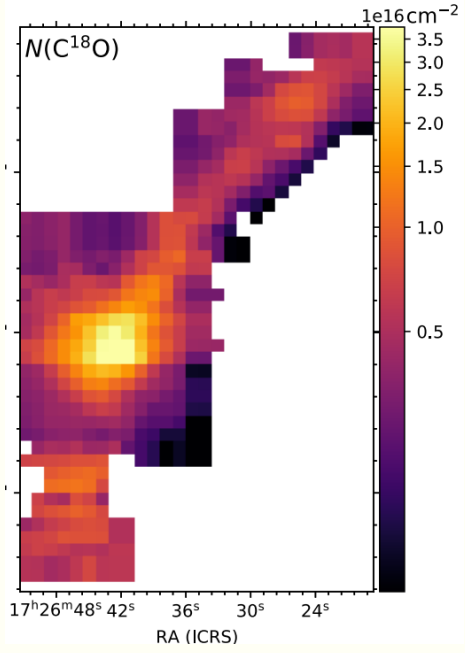

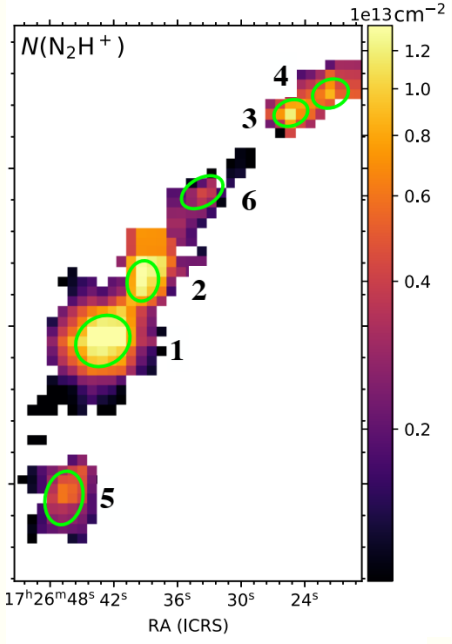

$N(C_{18}O)/N(H_2)$ = 2.0e-7を使ってH_2の柱密度を求める。

↓

- フィラメントの総質量 = 1800±50 [$M_\odot$]
- 線質量 = 529 [$M_\odot$/yr]

↕

- $M_{line,vir}$ = 512 [$M_\odot$/yr]

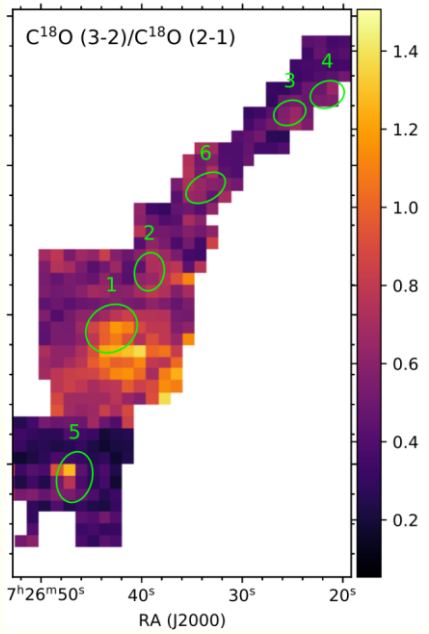

$$M_{\rm line,vir} = \left[1 + \left(\frac{\sigma_{\rm NT}}{c_{\rm s}}\right)^2\right] \times \left[16 M_\odot {\rm pc}^{-1} \times \left(\frac{T}{10{\rm K}}\right)\right], \quad (3)$$

where c_s is the sound speed, T is kinetic temperature and σ_{NT} is the non-thermal velocity dispersion, which is defined by:

$$\sigma_{\rm NT} = \sqrt{\frac{\Delta V^2}{8 \ln 2} - \frac{kT}{30 m_H}}, \quad (4)$$

where ΔV is the $C^{18}O$ line width, k is the Boltzmann constant, m_H is the mass of a hydrogen atom.

The virial parameter of the clumps $\alpha_{vir} = M_{vir}/M$ is calculated according to the definition in Kauffmann et al. (2013)

$$\alpha_{\rm vir} = \frac{5\sigma_v^2 R}{GM} = 1.2 \left(\frac{\sigma_v}{\rm km\ s^{-1}}\right)^2 \left(\frac{R}{\rm pc}\right) \left(\frac{M}{M_\odot}\right), \quad (4)$$

where σ_v is the velocity dispersion, R is the clump radius and G is the gravitational constant.

Clump	T, K Herschel	M, $M_\odot$	M_{vir}, $M_\odot$	α_{vir}
1	25	635 ± 25	889	1.4
2	18	173 ± 13	235	1.35
3	15	84 ± 9	130	1.55
4	14	57 ± 8	100	1.75
5	17	160 ± 13	121	0.76
6	14	77 ± 9	166	2.15

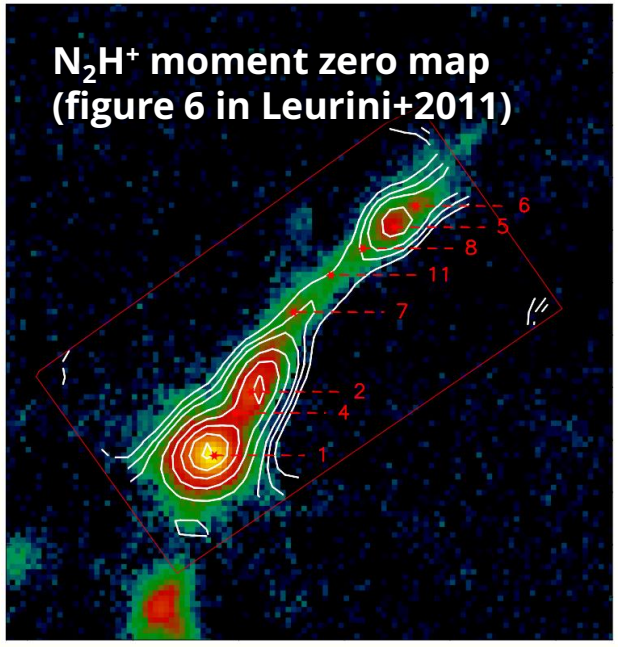
N_2H^+ moment zero map
(figure 6 in Leurini+2011)
6
5
8
11
7
2
4
1

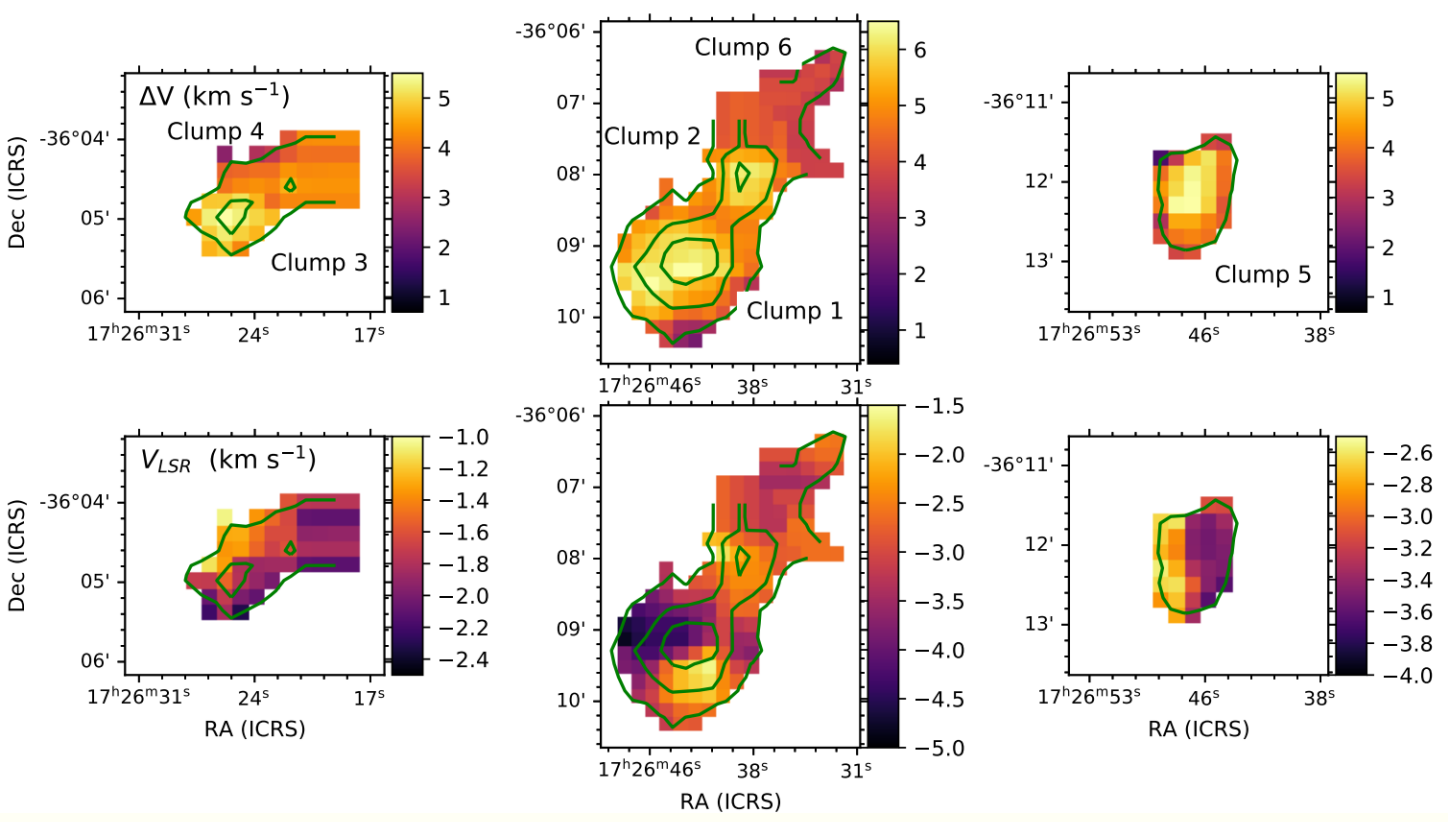
ΔV (km s^{-1})
Clump 4
Clump 3
Clump 6
Clump 2
Clump 1
Clump 5
V_{LSR} (km s^{-1})
Dec (ICRS)
RA (ICRS)
-36°04'
05'
06'
-36°06'
07'
08'
09'
10'
-36°11'
12'
13'
17^{h}26^{m}31^s
24^s
17^s
17^{h}26^{m}46^s
38^s
31^s
17^{h}26^{m}53^s
46^s
38^s

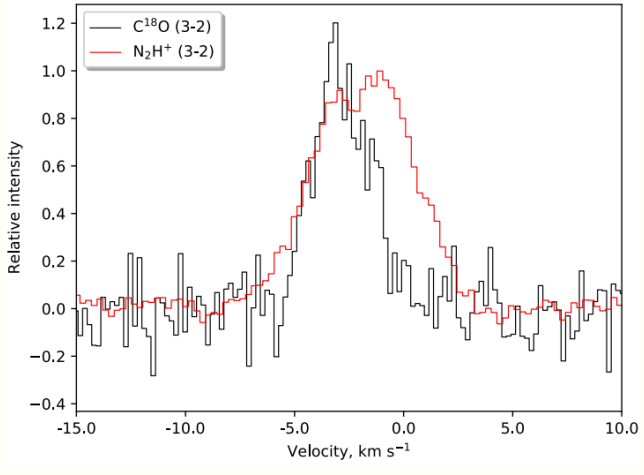
C^{18}O (3-2)
N_2H^+ (3-2)
Relative intensity
Velocity, km s^{-1}

Evolution of the atomic component in protostellar outflows

Show affiliations

Sperling, T. ; Eislöffel, J. ; Nisini, B. ; Giannini, T. ; Fischer, C. ; Krabbe, A.

We present SOFIA/FIFI-LS observations of three Class 0 and one Class I outflows (Cep E, HH 1, HH 212, and L1551 IRS5) in the far-infrared [O I]63mum and [O I]145mum transitions. Spectroscopic [O I]63mum maps enabled us to infer the spatial extent of warm, low-excitation atomic gas within these protostellar outflows. If proper shock conditions prevail, the instantaneous mass-ejection rate is directly connected to the [O I]63mum luminosity. In order to unravel evolutionary trends, we analysed a set of 14 Class 0/I outflow sources that were spatially resolved in the [O I]63mum emission. We compared these data with a sample of 72 Class 0/I/II outflow sources that have been observed with Herschel (WISH, DIGIT, WILL, GASPS surveys) without spatially resolving the [O I]63mum line.

Source	Class	Cloud	R.A. (J2000)[a] (h m s)	Decl. (J2000)[a] (° ′ ″)	D^b (pc)	$L_{bol}{}^c$ ($L_\odot$)	P.A.[h] (°)
IRAS 23011+6126 (Cep E)	0[g]	Cepheus, OB3	23 03 12.8	+61 42 26	730	~ 75[d]	25
VLA 1 (HH 1)	0[f]	Orion A, L1641	05 36 22.8	−06 46 06	430	~ 46[d]	145
IRAS 05413-0104 (HH 212)	0[g]	Orion B, L1630	05 43 51.4	−01 02 53	420	~ 13[d]	30
L1551 IRS 5	I[g]	Taurus, L1551	04 31 34.2	+18 08 05	140	~ 23[e]	75

天体：4 outflow sources

- 3 Class 0 (Cep E, HH1, HH212)
- 1 Class I (L1551 IRS 5)

観測装置：SOFIA / FIFI-LS

- During 2018 – 2019
- $[OI]_{63\mu m}$, $[OI]_{143\mu m}$

“Evolutionary indicator”

- **$f = (dM_{out}/dt)/(M_{acc}/dt)$**
- $f \sim 0.05 – 0.5$

72 Class 0/I/II 天体と比較

- low f (< 0.05) for Class 0 sources → underestimation the total Class 0 outflow mass

Object	Obs. date	Flight	Time[a] (min)	θ (°)	H (kft)	wvp (μm)
Cep E	2019-10-30	631	52	50	44	4.00
VLA 1, HH 1	2018-11-09	527	84	45	43	4.00
HH 212	2018-11-08	526	49	40	43	4.25
L1551IRS5	2019-11-07	637	21	45	43	4.50

航空機望遠鏡 SOFIA

- FIFI-LS (Far Infrared Field-Imaging Line Spectrometer)

4 天体を観測

- [OI]63.1837 μm, [OI]145.5254 μm
- 各アウトフロー軸に沿って駆動源近くまでマッピング

Class 0

Class 1

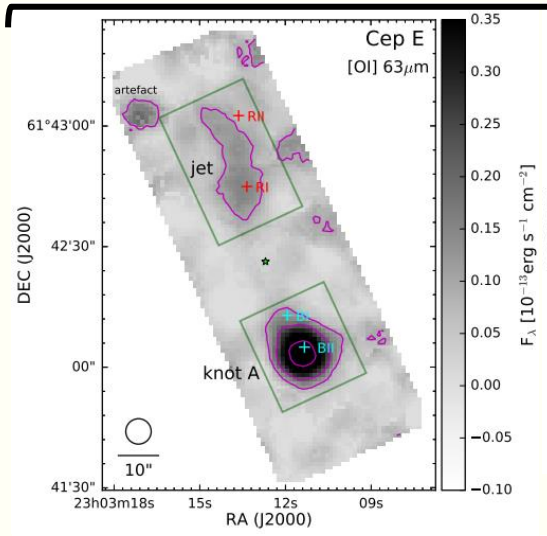

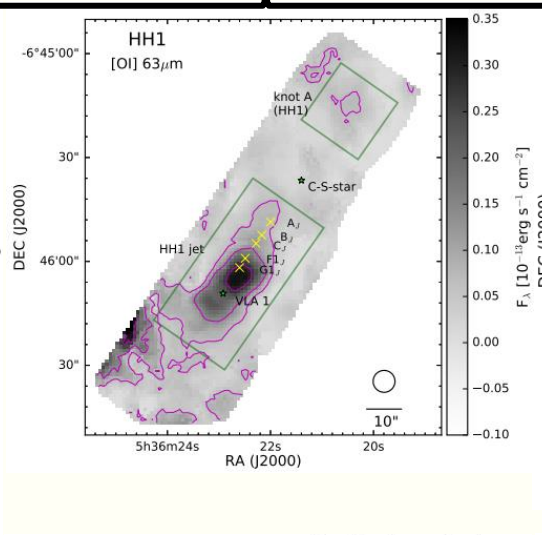

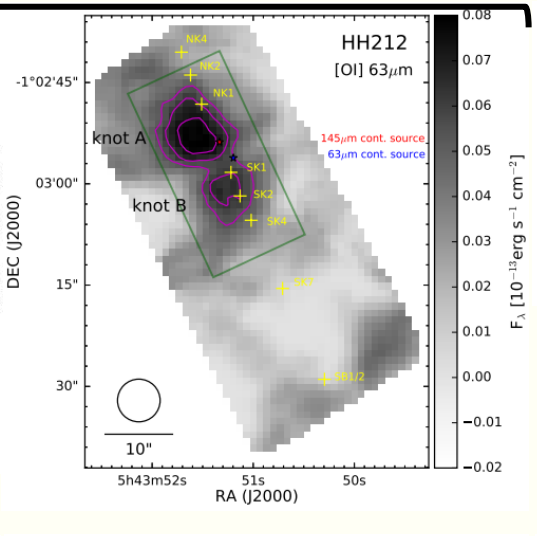

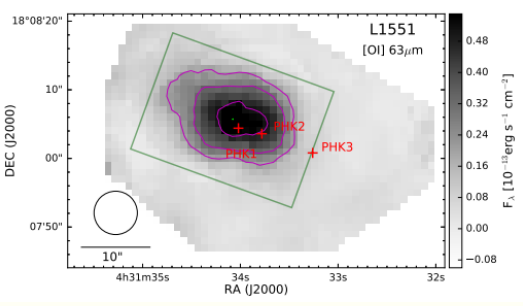

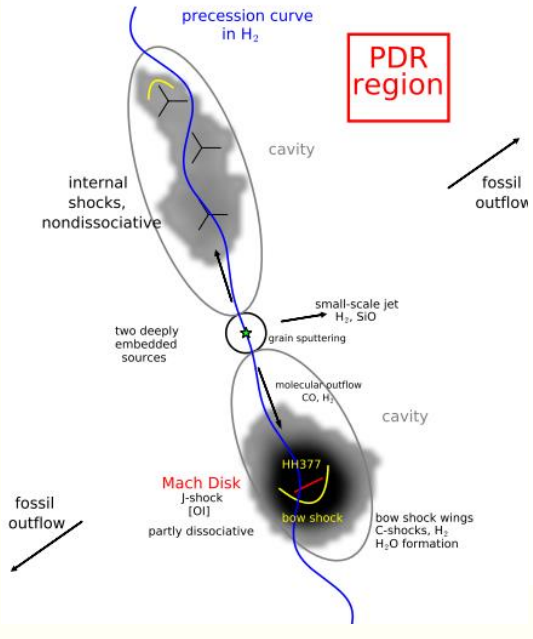

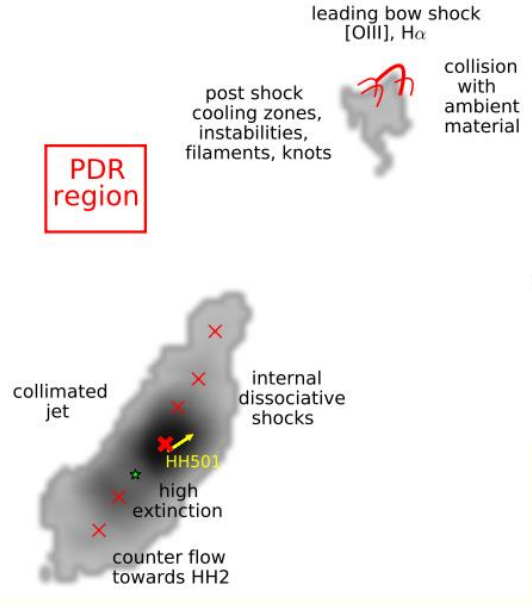

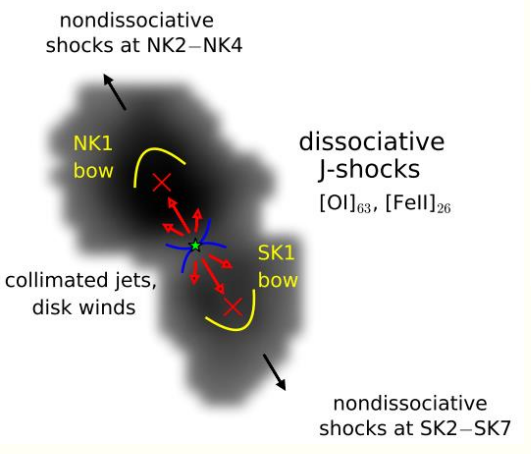

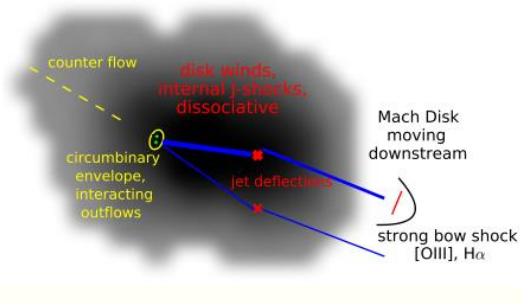

質量流出率 ... L([OI]$_{63}$) を用いて決定

(a) [OI]$_{63}$ lineでのジェット光度

$$\left(\frac{\dot{M}_{\rm out}^{\rm lum}}{M_\odot\,{\rm yr}^{-1}}\right) = (3.3-6.7)\times10^{-3}\cdot\left(\frac{v_{\rm t}}{{\rm km\,s}^{-1}}\right)\left(\frac{''}{\theta}\right)\left(\frac{\rm pc}{D}\right)\left(\frac{L([{\rm O\,I}]_{63})}{L_\odot}\right)$$

(vt ... ジェット速度, θ ... ジェット角, D ... ジェットまでの距離)

(b) 衝撃波モデル (Hollembach & McKee 1989; HM89)

$$\dot{M}_{\rm out}^{\rm shock} = 10^{-4}\,L([{\rm O\,I}]_{63})/L_\odot\,M_\odot\,{\rm yr}^{-1}$$

質量降着率 ... $L_{\rm acc}$, L_*, M_* を用いて決定

$$\dot{M}_{\rm acc} = \frac{L_{\rm acc}R_\star}{GM_\star}$$

Class 0: $M_\star = 0.2\,M_\odot$, $R_\star = 4\,R_\odot$, $L_{\rm acc} = L_{\rm bol}$
Class I: $M_\star = 0.5\,M_\odot$, $R_\star = 4\,R_\odot$, $L_{\rm acc} = 0.5L_{\rm bol}$

$$\left(\frac{\dot{M}_{\rm acc}}{10^{-6}\,M_\odot\,{\rm yr}^{-1}}\right) \approx \frac{1}{3.1\,f_{\rm acc}}\left(\frac{0.25\,M_\odot}{M_\star}\right)\left(\frac{R_\star}{2.5\,R_\odot}\right)\left(\frac{L_{\rm acc}}{L_\odot}\right)$$

(中間質量星Cep Eのみ別式で計算)

Obj.	Region	θ (")	v_t (km s^{-1})	$\dot{M}_{out}^{lum}$([O I]) (10^{-7} $M_\odot$ yr^{-1})	$\dot{M}_{out}^{shock}$([O I]) (10^{-7} $M_\odot$ yr^{-1})	$\dot{M}_{out}^{other}$ & component (10^{-7} $M_\odot$ yr^{-1})	$\dot{M}_{acc}$ [e] (10^{-7} $M_\odot$ yr^{-1})
Cep E	knot A	25	95[a]	$\lesssim$ 22.4 – 45.5	$\lesssim$ 124.4 – 136.7	~ 200[j] & CO	170[f]
	jet	35	60[a]	$\lesssim$ 7.2 – 14.7	$\lesssim$ 87.5 – 99.0		
HH 1	VLA 1	50	300[b]	$\lesssim$ 25.9 – 52.6	$\lesssim$ 54.9 – 57.8	~ 6[k] & [Fe II]	290[g]
	knot A	20	400[b]	$\lesssim$ 9.5 – 19.4	$\lesssim$ 5.2 – 7.2	~ 4[k] & [S II]	
						~ 0.1[k] & H_2	
						~ 15[l] & CO	
HH 212	knots A and B	30	150[c]	3.9 – 7.9	8.0 – 11.8	~ 10[m] & CO, SO, SiO	80[h]
						$\leq$ 3[n] & CO, SiO	
						~ 1[o] & H_2	
L1551	IRS 5	25	120[d]	5.8 – 11.8	4.9 – 5.4	$\gtrsim$ 100[p] & CO, HCO^+, swept-up gas	30[i]
						~ 8.6[q] & HI	
						~ 1.7[r] & [Fe II]	
						~ 0.4[r] & H_2	

7列目のデータ ... 他の輝線観測から求めた質量流出率

- Cep E　　：[OI]から求めた値より高い → ジェットの大部分は分子
- HH1・HH212：[OI]から求めた値より低い → ジェットは低励起原子が主
- L1551　　：[OI]から求めた値とコンパラ → 原子成分が分子と同程度に重要

Source	Class	D (pc)	θ (")	v_t (km s^{-1})	L([O I]) $L_\odot$	$\dot{M}_{out}^{lum}$([O I]) (10^{-7} $M_\odot$ yr^{-1})	$\dot{M}_{out}^{shock}$([O I]) (10^{-7} $M_\odot$ yr^{-1})	$\dot{M}_{other}$ & component	$\dot{M}_{acc}$[a] (10^{-7} $M_\odot$ yr^{-1})	Main ref.
HH 111 IRS	I	420	20	270	2.5×10^{-2}	26 – 53	22.9 – 26.4	4 & CO[b]	27[k]	Sperling et al. (2020)
HH 111 jet		420	45	260	1.3×10^{-2}	6 – 12	$\lesssim$ 10 – 16	2 – 6 & [O I]λ6300[r]		
SVS13A	I	235	22	270	1.5×10^{-2}	25 – 51	13.1 – 16.0	8.9 & [Fe II][c] 7.0 & H_2[c] 30 & HI[d] 90 & low-J CO[e], swept-up gas	140 – 170[l]	Sperling et al. (2020)
HH 34 IRS	I	430	26	160	2.4×10^{-2}	11 – 23	20.7 – 27.5	0.7 & [Fe II][c] 0.03 & H_2[c] $\sim$ 1.5 & [O I]λ6300[r]	35 – 115[m]	Sperling et al. (2020)
L1448-C	0	232	45	170	1.8×10^{-3}	1 – 2	2 – 4	$\sim$ 24 & SiO, SO, CO[f]	35	Nisini et al. (2015)
IRAS4A	0	235	38	100 – 140	9.1×10^{-4}	0.3 – 1.0	1 – 2	$\gtrsim$ 18 & SiO, SO, CO[g]	58	Nisini et al. (2015)
HH 46	I	450	59	300	2.0×10^{-2}	7 – 15	20 – 40	15 – 28 & CO[v]	34[n]	Nisini et al. (2015)
BHR 71	0	200	33	50 – 100	3.2×10^{-3}	1 – 3	3 – 6	21 & CO[t]	73[o]	Nisini et al. (2015)
VLA 1623	0	120	78	60	2.1×10^{-3}	0.5 – 1	2 – 4	16 – 160 & CO	21	Nisini et al. (2015)
HH 211 SE lobe	0	250	51	115	3.92×10^{-3}	1.2 – 2.4	3.9			
HH 211 NW lobe	0	250	45	115	3.57×10^{-3}	1.2 – 2.4	3.6			
HH 211 both lobes						2.4 – 4.8	7.5	7 – 28 & SiO, CO, SO[h] $\sim$ 20 – 28 & H_2[i]	14[p]	Dionatos et al. (2018)
IRAS 2A, blue lobe SN	0	235	188	50	3.5×10^{-3}	0.1 – 0.3	3.5	200 & CO[u]		
IRAS 2A, red lobe SN	0	235	133	50	4.1×10^{-3}	0.2 – 0.4	4.1	400 & CO[u]		
IRAS 2A, both lobes SN						0.3 – 0.7	7.6	6 & H_2[j] > 6.7 & SiO, SO, CO[s]	234[q]	Dionatos & Güdel (2017)

14 天体 (高分解能観測)

72 天体 (低分解能観測を含める)

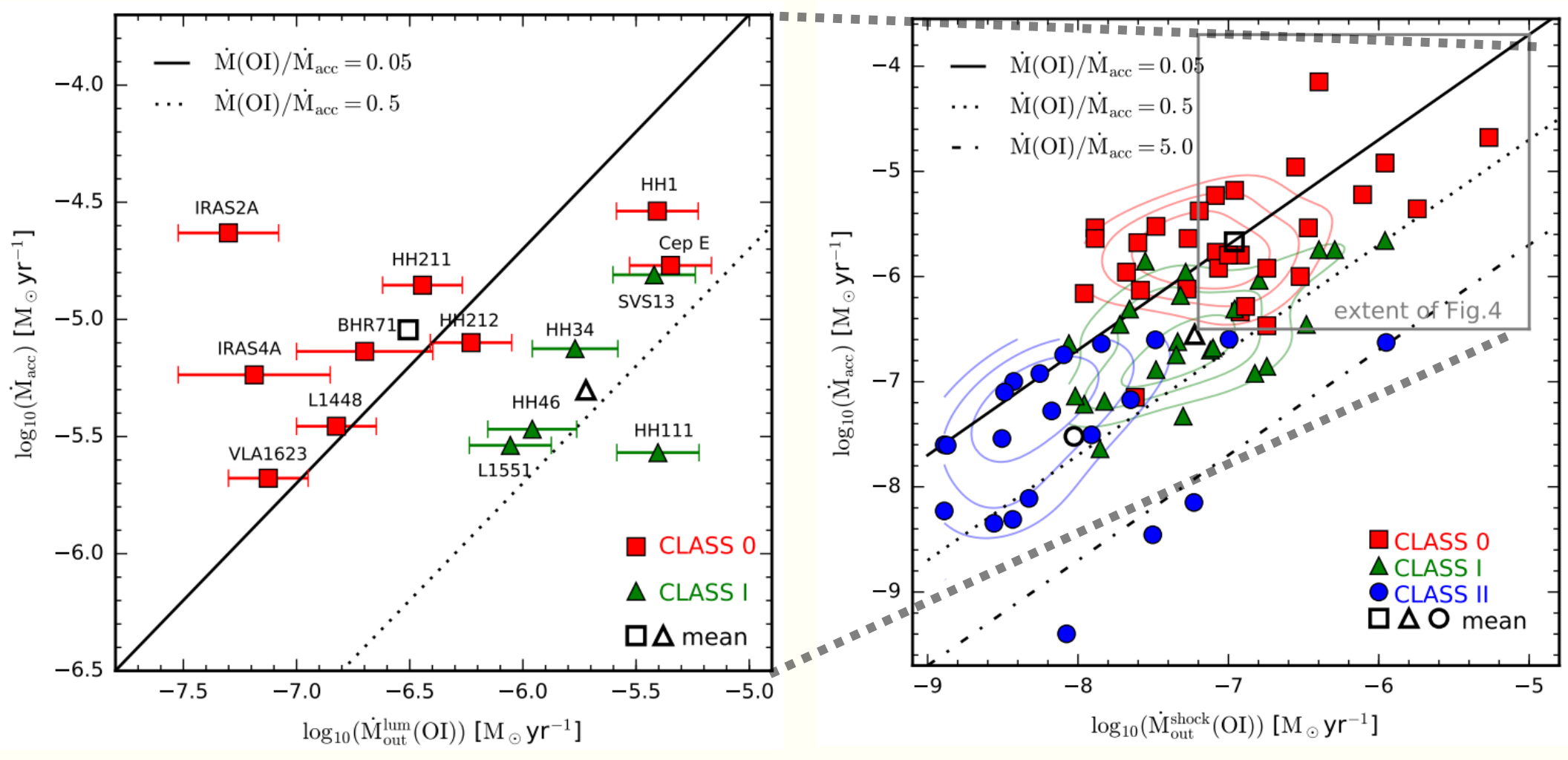

A study of the photometric and spectroscopic variations of the prototypical FU Orionis-type star V1057 Cyg

Show affiliations | Hide authors

Szabó, Zs. M. ; Kóspál, Á. ; Ábrahám, P. ; Park, S. ; Siwak, M. ; Green, J. D. ; Moór, A. ; Pál, A. ; Acosta-Pulido, J. A. ; Lee, J. -E. ; Cseh, B. ; Csörnyei, G. ; Hanyecz, O. ; Könyves-Tóth, R. ; Krezinger, M. ; Kriskovics, L. ; Ordasi, A. ; Sárneczky, K. ; Seli, B. ; Szakáts, R. Szing, A. ; Vida, K.

Among the low-mass pre-main sequence stars, a small group called FU Orionis-type objects (FUors) are notable for undergoing powerful accretion outbursts. V1057 Cyg, a classical example of an FUor, went into outburst around 1969-1970, after which it faded rapidly, making it the fastest fading FUor known. Around 1995, a more rapid increase in fading occurred. Since that time, strong photometric modulations have been present. We present nearly 10 years of source monitoring at Piszkéstető Observatory, complemented with optical/near-infrared photometry and spectroscopy from the Nordic Optical Telescope, Bohyunsan Optical Astronomy Observatory, Transiting Exoplanet Survey Satellite, and the Stratospheric Observatory for Infrared Astronomy. Our light curves show continuation of significant quasi-periodic variability in brightness over the past decade. Our spectroscopic observations show strong wind features, shell features, and forbidden emission lines. All of these spectral lines vary with time. We also report the first detection of [S II], [N II], and [O III] lines in the star.

Target: V1057 Cyg

- Classical FU Orionis-type object

Inst.:

- Monitoring between 2012 – 2020

Long-term photometric monitoring

- Find 2nd photometric plateau
- 2 periods
- t_{period} = 502±20 [days] → (起源) 星から1 [au]に位置する3500–4000 [K]に加熱された0.3×0.2 [au]のbubble
- t_{period} = 1707±70 [days] → (起源) エンベロープから円盤に落下したダストによる、円盤中心部の周期的な掩蔽
- V1057 Cygはまだアウトバースト中

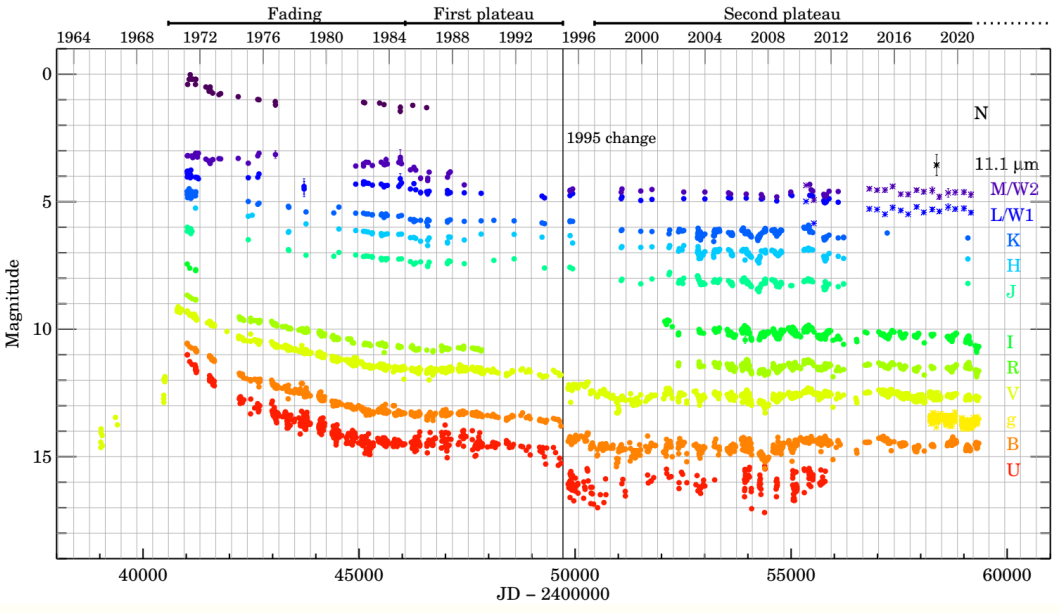

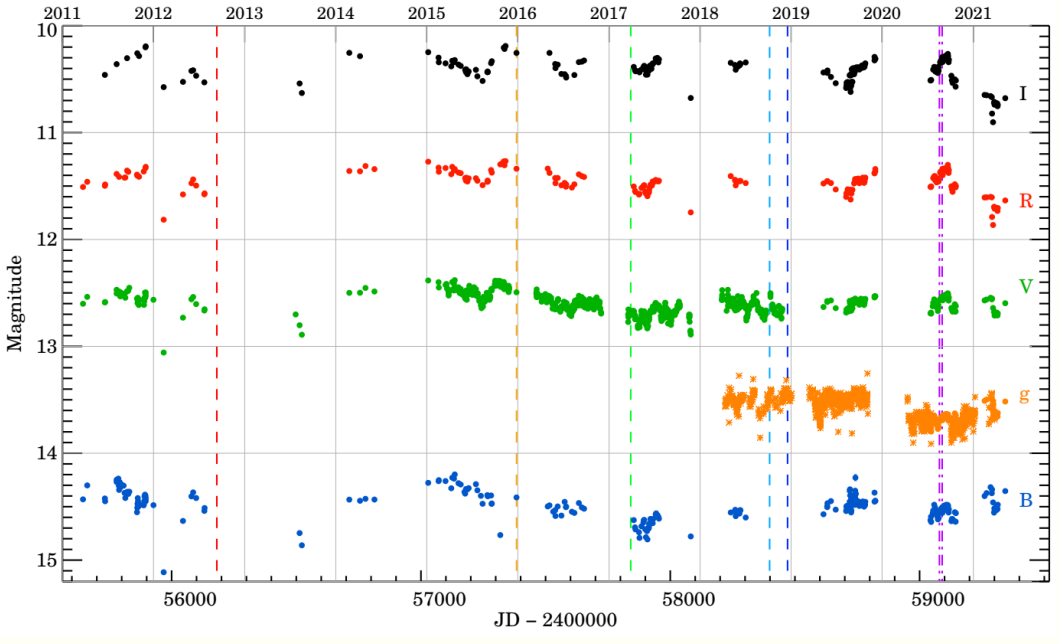

Date	Filters	Status of the source	Ref.
1971	$JHKL$	Main fading phase	1
1971	$UBVRI$	Main fading phase	2
1971	$JHKLMN$	Main fading phase	2
1975	UBV	Main fading phase	3
1976	UBV	Main fading phase	4
1971–1974	UBV	Main fading phase	5
1971–1974	MN	Main fading phase	6
1975–1977	UBV	Main fading phase	7
1981	$JHKLMN$	Main fading phase	8
1971–1987	$JHKLMN$	Fading & First plateau	9
1989–1991	KMN	First plateau	10
1985–2011	$UBVR$	First & Second plateau	11
1985–2011	$JHKLM$	First & Second plateau	11
2005–2007	BVR_CI_C	Second plateau	This work
2011–2019	BVR_CI_C	Second plateau	This work
2019–2020	$BVg'r'i'$	Second plateau	This work
2006, 2012	BVR_JI_J	Second plateau	This work
2020	$BVRi^a$	Second plateau	This work
2019	TESS I	Second plateau	This work
2006, 2012	JHK_s	Second plateau	This work
2020	JHK_s	Second plateau	This work

The *Gaia* view of the Cepheus flare

Show affiliations

Szilágyi, Máté ; Kun, Mária ; Ábrahám, Péter

We present a new census of candidate pre-main-sequence stars in the Cepheus flare star-forming region, based on *Gaia* EDR3 parallaxes, proper motions, and colour—magnitude diagrams. We identified new candidate members of the previously known young stellar groups associated with NGC 7023, L1177, L1217/L1219, L1228, L1235, and L1251. We studied the 3D structure of the star-forming complex and the distribution of tangential velocities of the young stars. The young stellar groups are located between 330 and 368 pc from the Sun, divide into three kinematic subgroups, and have ages between 1—5 million years. The results confirm the scenario of propagating star formation, suggested by previous studies. In addition to the bulk pre-main-sequence star population between 330 and 370 pc, there is a scattered and more evolved pre-main-sequence population around 150—180 pc. We found new candidate members of the nearby Cepheus Association, and identified a new moving group of 46, 15—20 million years old pre-main-sequence stars located at a distance of 178 pc, around the A0-type star HD 190833. A few pre-main-sequence stars are located at 800—900 pc, indicative of star-forming regions associated with the Galactic local arm above the Galactic latitude of +10°.

Molecular Cloud Cores with High Deuterium Fractions: Nobeyama Mapping Survey

Show affiliations | Hide authors

Tatematsu, Ken'ichi ; Kim, Gwanjeong ; Liu, Tie ; Evans, Neal J., II ; Yi, Hee-Weon ; Lee, Jeong-Eun ; Wu, Yuefang ; Hirano, Naomi ; Liu, Sheng-Yuan ; Dutta, Somnath ; Sahu, Dipen ; Sanhueza, Patricio ; Kim, Kee-Tae ; Juvela, Mika ; T'oth, L. Viktor ; Feh'er, Orsolya ; He, Jinhua ; Ge, J. X. ; Feng, Siyi ; Choi, Minho Kang, Miju ; Thompson, Mark A. ; Fuller, Gary A. ; Li, Di ; Ristorcelli, Isabelle ; Wang, Ke ; Di Francesco, James ; Eden, David ; Ohashi, Satoshi ; Kandori, Ryo ; Vastel, Charlotte ; Hirota, Tomoya ; Sakai, Takeshi ; Lu, Xing ; Nguyen Lu'o'ng, Quang ; Shinnaga, Hiroko ; Kim, Jungha ; JCMT Large Program "SCOPE" collaboration

We present the results of on-the-fly mapping observations of 44 fields containing 107 SCUBA-2 cores in the emission lines of molecules, N_2H^+, HC_3N, and CCS at 82—94 GHz using the Nobeyama 45-m telescope. This study aimed at investigating the physical properties of cores that show high deuterium fractions and might be close to the onset of star formation. We found that the distributions of the N_2H^+ and HC_3N line emissions are approximately similar to that of 850-μm dust continuum emission, whereas the CCS line emission is often undetected or is distributed in a clumpy structure surrounding the peak position of the 850-μm dust continuum emission. Occasionally (12%), we observe the CCS emission which is an early-type gas tracer toward the young stellar object, probably due to local high excitation. Evolution toward star formation does not immediately affect nonthermal velocity dispersion.